Direct Observation of Charge Density Wave Current Conversion by Spatially Resolved Synchrotron X-Ray Studies in $NbSe_3$

H. Requardt,[1,2] F. Ya. Nad,[1,3] P. Monceau,[1] R. Currat,[2] J. E. Lorenzo,[4] S. Brazovskii,[2,5,6,7]
N. Kirova,[7] G. Grübel,[6] and Ch. Vettier[6]
[1]*Centre de Recherches sur les Très Basses Températures, CNRS, B.P. 166, 38042 Grenoble, France*
[2]*Institut Laue Langevin, B.P. 156, 38042 Grenoble, France*
[3]*Institute of Radio-Engineering and Electronics, 103907 Moscow, Russia*
[4]*Laboratoire de Cristallographie, CNRS, B.P. 166, 38042 Grenoble, France*
[5]*Landau Institute, Moscow, Russia*
[6]*European Synchrotron Radiation Facility, B.P. 220, 38043 Grenoble, France*
[7]*Los Alamos National Laboratory, Los Alamos, New Mexico 87545*
(Received 18 February 1998)

We present results on the normal-collective current conversion processes and associated deformation profile for a charge density wave in the sliding state. High resolution x-ray measurements of the satellite positional shift have been performed on $NbSe_3$ at 90 K. The shift q has been determined in the vicinity of the contacts by applying direct currents. We observe a steep variation of q near the contact, modeled in terms of dislocation loops (DL) nucleated at host defects. A small constant gradient in the sample's central part indicates incomplete conversion, consistent with DL pinning. [S0031-9007(98)06427-8]

PACS numbers: 71.45.Lr, 61.10.–i, 72.15.Nj

Phase slippage is a common phenomenon [1] in condensed matter systems with complex order parameters. Phase gradients in the condensate, as originating, e.g., from external forces, cannot grow indefinitely. Beyond some critical value, the strain associated with the phase gradient is released through 2π-phase jumps. The process is repetitive in time, with a rate dependent on the magnitude of the external force. Phase slippage has been intensively studied in narrow superconducting channels [2,3], in superfluid helium [4], and in quasi-one-dimensional charge density wave (CDW) systems.

In the latter case, below the Peierls transition temperature T_P, the system is characterized by a modulated electronic density: $\rho(x) = \rho_0[1 + \alpha\cos(Q_0x + \varphi)]$ together with a periodic lattice distortion of the same wavelength, $2\pi/Q_0 = 2\pi/2k_F$ where k_F is the (generally incommensurate) Fermi momentum. The new periodicity opens a gap in the electron density of states and leads to new (satellite) Bragg peaks. CDW pinning by host defects fixes the local phase φ and destroys the translational invariance of the CDW ground state. Application of an electric field $\mathcal{E}$ above a threshold value $\mathcal{E}_T$, sets the CDW in motion and gives rise to a collective current [5–7].

Phase slippage is required at the electrodes for the conversion from free to condensed carriers [8–10]. When the CDW is depinned between current contacts, CDW wave fronts are created near one electrode and destroyed near the other, leading to CDW compression at one end and stretching at the other end. In a purely 1D channel, the order parameter is driven to zero at a distance x_0 from the pinning ends [8]. For samples of finite cross section, phase slippage develops as dislocation loops (DL) which climb to the crystal surface, each DL allowing the CDW to progress by one wavelength [9].

Local CDW deformations under the influence of an electric field have been studied by several *indirect* methods [11], such as measurements of the shift of the local chemical potential along the sample using a laser probe [12], electromodulated IR transmission [13], and conductivity measurements on multicontacted samples [14–16]. On the other hand, x-ray measurements yield *direct* information on the spatial distribution of the CDW deformations. So far, a single experiment has been reported on $NbSe_3$ [17]: the CDW deformation was monitored using a 0.8-mm-wide x-ray beam on a 4.5-mm-long sample. The data in Ref. [17] suggest an approximately linear variation of the satellite shift with x in the central part of the sample, but experimental limitations did not allow the contact regions to be investigated.

Hereafter we report high resolution x-ray scattering measurements of the variation $q(x)$ of the CDW wave vector $Q(x) = Q_0 + q(x)$ of $NbSe_3$ along the sample length with special emphasis on the near-contact region. The measurements have been carried out on the diffractometer TROIKA I (ID 10A) at ESRF (Grenoble/France) using an incident wavelength of 1.127 Å ($E = 11$ keV), provided by a single Si(111) monochromator. High spatial resolution was obtained by reducing the beam width to 100 μm, down to 30 μm in the vicinity of the contacts.

The required Q-space resolution was obtained by using detector slits of 100 μm width, yielding a longitudinal resolution $\delta Q = 6.8 \times 10^{-4}$ Å^{-1} at the (020) Bragg reflection of the sample. The mosaicity of the sample was found to be about 0.015°. The sample was oriented with the $(\mathbf{a}^* + \mathbf{c}^*, \mathbf{b}^*)$ plane as the horizontal scattering plane. All measurements were carried out at $T = 90$ K, in the upper CDW state ($T_{P_1} = 145$ K; $Q_0 = 0.241b^*$) corresponding to the Peierls condensation of type-III chains

[18]. A sample of cross section $10 \times 2\ \mu m^2$ was mounted on a 100-μm-thick sapphire substrate, providing homogeneous sample cooling as well as adequate beam transmission (~50%). Electrical contacts were prepared by evaporating wide, 2-μm-thick gold layers onto the sample, leaving a free sample length of 4.1 mm between electrodes. The use of a substrate and the comparably low threshold current value ($I_T = 2.16$ mA) allowed measurements to be performed not only with pulsed currents (pc) (100 Hz, 1% duty cycle) but also with direct currents (dc) up to 8 mA ($= 3.7 I_T$) without signs of Ohmic heating.

To erase any remnant deformation due to sample history, we applied a procedure analogous to that used in demagnetization or depolarization techniques, i.e., application of currents of alternating polarities and decreasing amplitude. We verified (see Fig. 1) that this technique succeeds in recovering the original *zero-field* satellite position as well as the corresponding profile widths, along $\mathbf{b}^*$ and perpendicular to the chain direction (rocking width).

Figure 2 shows the shift q of the $(0, 1 + Q_0, 0)$ CDW satellite using both pc and dc applied currents up to $I/I_T = 4$. The x-ray beam is positioned 100 μm away from the current injection contact. In both cases, a shift of the CDW satellite wave vector is observed for currents exceeding I_T. The shift q increases rapidly with I/I_T but saturates at higher currents. For pc and dc, 90% of the saturation value is achieved at $|I| = 2I_T$. This behavior is in good agreement with similar results in Ref. [17]. Here we find, additionally, that the application of a dc current produces a larger shift ($\sim \times 1.7$) than a pulsed current of the same intensity.

Figure 3 shows the "double-shift" $q_\pm = Q(+I) - Q(-I)$ as a function of beam position x along the left-hand half of the sample ($0 < x < 2$) for applied (pc and dc) currents of $|I| = 4.6$ mA $= 2.13 I_T$. For both types of current, $q_\pm(x)$ shows a linear variation with position x in the middle section of the sample ($0.7 < x < 2.0$), and no difference is observed between direct and pulsed currents. Closer to the contact ($0 < x < 0.7$), $q_\pm(x)$ deviates from linearity: the dc shift increases more rapidly than the pc shift and reaches its maximum *at* the contact boundary, while the maximum pc shift occurs at a distance of about 100 μm *away* from the contact boundary. These differences suggest a spatially dependent, relaxational behavior for the CDW deformations, the fastest relaxation occurring at the contact position. A linear fit of the data in the region $0.7 < x < 2.0$ yields a slope $\partial(q_\pm)/\partial x = -(2.0 \pm 0.1) \times 10^{-4} b^*$.

The accepted interpretation of the CDW distortions associated with current injection follows the argument [17,19] that the energy $\propto U^* q$ of the distortion q observed at some effective stress U^* is opposed by the elastic energy $\propto K q^2$, resulting in $q \propto -U^*/K$. For a simple 1D case, a constant gradient $\partial q/\partial x = q_0' \neq 0$ is obtained. The large discrepancy between the present results and the strain profile obtained from the models in [16] and [19] calls for a new theoretical approach (a detailed account of the model presented below will be published elsewhere [20]).

In $NbSe_3$, in the upper CDW state, there are two types $\alpha = i, e$ of normal carriers. The intrinsic carriers, $\alpha = i$, originate from the condensed bands with metallic state Fermi level density of states N_F^i. At $T = 90$ K, they are excited across the Peierls gap. The extrinsic carriers (N_F^e) arise from uncondensed bands (on type-I and type-II chains [18]). In the condensed state, the potential V_α experienced by the carriers is $V_e = \Phi$ and $V_i = V = \Phi + q/\pi N_F^i$, with Φ the electric potential [21]. The electrochemical potentials are $\mu_\alpha \approx V_\alpha + \delta n_\alpha/\rho_\alpha N_F^\alpha$, where δn_α is the local imbalance between electron and hole concentrations for each carrier type α. The relative "normal density" $\rho_i(T)$ and the relative "condensate density" [21]

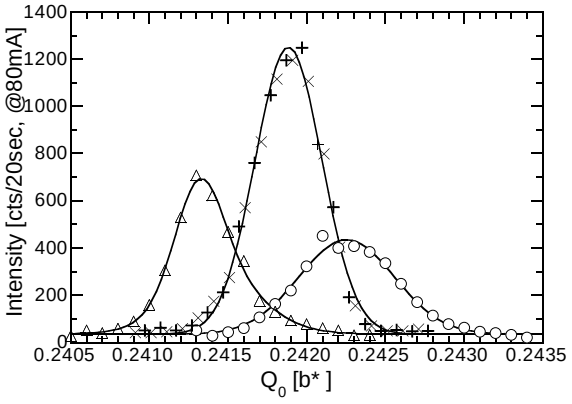

FIG. 1. Longitudinal satellite profiles at $x = 100$ μm: (+) $I_{dc} = 0$, (○) $I_{dc} = 2.13 I_T$, (×) $I_{dc} = 0$ after depolarization, and (△) $I_{dc} = -2.13 I_T$; $NbSe_3$, $T = 90$ K.

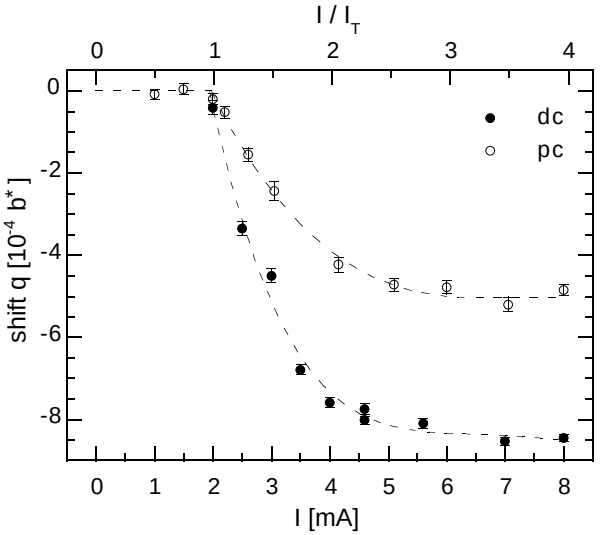

FIG. 2. Change of satellite position, q, for pulsed (100 Hz, 1% duty cycle) (○) and direct currents (●) of varying intensities. The measurements are performed at a distance of 100 μm from the current injection contact. Beam width: 100 μm; $NbSe_3$, $T = 90$ K; dashed lines are guides for the eye.

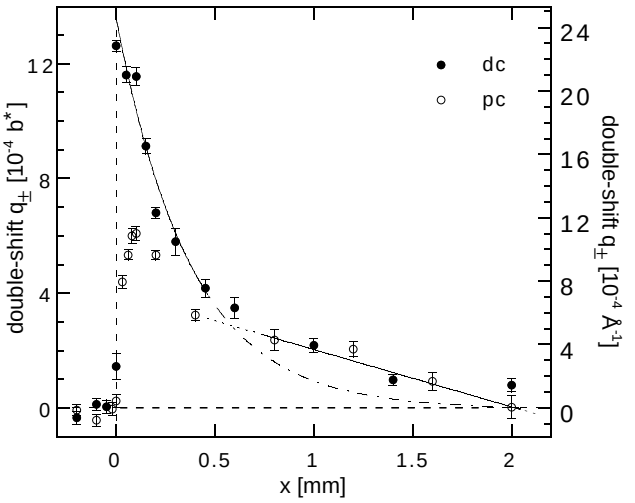

FIG. 3. Double-shift $q_\pm(x) = Q(+I) - Q(-I)$ (in units of $\mathbf{b}^*$) for direct (●) and pulsed (○) current ($I/I_T = 2.13$). The full line shows the exponential fit from Eq. (4) near the contact ($0 < x < 0.5$) and a linear dependence for $0.7 < x < 2$. The dash-dotted line extrapolates the exponential fit into the central section. The vertical dashed line represents the contact boundary; the horizontal dashed line, the line of zero shift. $NbSe_3$, $T = 90$ K.

$\rho_c(T) = 1 - \rho_i(T)$ change from $\rho_i = 1$, $\rho_c = 0$ in the metallic state to $\rho_i = 0$, $\rho_c = 1$ at low T. At the same time $\rho_e \approx 1$ stays constant (until the second CDW transition at $T_{P_2} = 59$ K). Fast equilibration of quasiparticles always leads locally to $\mu_i = \mu_e \equiv \mu_n$. The inhomogeneous electrochemical potential μ_n determines the normal current $j_n = -\sigma_n \partial\mu_n/\partial x$, where $\sigma_n = \sigma_i + \sigma_e$ is the normal conductivity.

We separate the total charge density δn_{tot} and current density j_{tot} into their normal and condensate counterparts, $\delta n_{\text{tot}} = \delta n_n + \delta n_c$ and $j_{\text{tot}} = j_n + j_c$, with $\delta n_n = \delta n_e + \delta n_i$, $\delta n_c = \varphi_x/\pi$, and $j_c = -\varphi_t/\pi$; $\varphi_x = \partial\varphi/\partial x = q$ and $\varphi_t = \partial\varphi/\partial t$ stand for the local space and time derivatives of the CDW phase φ. We define the longitudinal CDW stress $2U$ as the energy per chain paid to distort the CDW elastically by one period. U, as well as the strain q/π, refer to one electron in the ground state. With this choice, U and the CDW driving force $\mathcal{F} = -\partial U/\partial x$ are additive to Φ and $\mathcal{E} = -\partial\Phi/\partial x$, respectively. U includes contributions from three sources: the elastic stress, the stress provided by the excess concentration of intrinsic carriers, and the electric potential,

$$U = (q/\pi + \delta n_i)/N_F^i + \Phi\,. \tag{1}$$

The force $\mathcal{F}$ is equilibrated either by the rest pinning force $\mathcal{F}_{\text{pin}}$ for $\mathcal{E} < \mathcal{E}_T$ or by the friction force $\mathcal{F}_{\text{frc}}(j_c)$ for $\mathcal{E} > \mathcal{E}_T$. The equation $\mathcal{F} = -\mathcal{F}_{\text{frc}}(j_c)$ and its inverse $j_c = J_c(\mathcal{F})$ are obtained from the V-I or I-V characteristics of the sliding CDW.

The local electroneutrality condition [22] implies that the variation of the carrier concentration δn_n images the CDW wave number variations [12]: $\delta n_n = -\delta n_c = -q/\pi$. With this relation and expressions for V and U, we can express q, at any x and t, as

$$gq/\pi N_F^i = \mu_n - U \equiv \eta\,, \tag{2}$$

with $g = 1/(g_i^{-1} + \beta_e)$, $g_i = (1 - \rho_i)/\rho_i$. β_e characterizes the screening of the CDW deformations by the extrinsic carriers. g is the normalized elastic constant since the total static energy density of the strained state is $(K/2)(\varphi_x/\pi)^2$ with $K = g/N_F^i$. We see that the CDW is deformed whenever the stress U does not coincide with the electrochemical potential of the normal carriers μ_n. The quantity η measures this mismatch, and hence characterizes the excess or lack of normal carriers, which is measured directly by q. The exchange between the normal carriers and the condensate results finally in the equilibration between μ_n and U, a process taking place via nucleation and growth of DLs.

Equation (2) must be supplied with boundary conditions and with a law for the current conversion due to DL nucleation. At the contacts $x = \pm a$: $j_n(\pm a) = j_{\text{tot}}$, $j_c(\pm a) = 0$. The second condition, far from the contacts, distinguishes our picture from other recent treatments, e.g., [19]: the condition that *all partial currents are stationary in the sample bulk* implies the *absence of current conversion,* all types of carriers being in equilibrium, with *equal chemical potentials.*

The balance between the different types of carriers is controlled by the injection and extraction rates from the electrodes and by the conversion rate $\mathcal{R}$ between normal and condensed carriers. The stationary distribution of the CDW deformation is obtained from Eq. (2) as

$$\frac{\partial\eta}{\partial x} = \frac{\partial\mu_n}{\partial x} - \frac{\partial U}{\partial x} = \mathcal{F}(j_c) - \frac{j_{\text{tot}}}{\sigma_n} + \frac{j_c}{\sigma_n}\,, \tag{3}$$

which follows from the definition of U and the current partition $j_n = j_{\text{tot}} - j_c$. Equation (3) should be combined with the relation $\partial j_c/\partial x = \mathcal{R}(\eta, j_c)$ which results from the carrier conservation law $\partial(\delta n_c)/\partial t + \partial j_c/\partial x = d(\delta n_c)/dt = \mathcal{R}$ with $\partial(\delta n_c)/\partial t = 0$ in the stationary case.

There are two extreme scenarios for $\mathcal{R}(\eta)$. The first refers to an ideal host crystal, both in the bulk and at the surface, where only homogeneous nucleation is present as a spontaneous thermal [19] or even quantum [23] supercritical fluctuation, so that $\mathcal{R} \propto \exp(-\eta_0/|\eta|)$, valid at $|\eta| \ll \eta_0$. Another extreme refers to samples with a sufficiently large density of defects acting as nucleation centers for supercritical DLs, the simplest form for this case being $\mathcal{R} \propto \eta$. Both scenarios are of the "passive" type, when the CDW motion itself plays no role.

A plausible "active" scenario emerges for a fast enough CDW motion when the DLs are created by the CDW sliding through bulk or surface defects: $\mathcal{R} = \mathcal{R}(\eta, j_c)$ such that $\mathcal{R}(0, j_c) = \mathcal{R}(\eta, 0) = 0$ with $\mathcal{R} \propto \eta j_c$ as the simplest version.

For homogeneous nucleation, with $\mathcal{R} \propto \exp(-\eta_0/|\eta|)$ we find $q \propto (\ln|x - a|)^{-1}$. This is an extremely slow decrease, which results in an incomplete carrier conversion and a large linear gradient across the *finite* sample length.

Assuming heterogeneous, passive nucleation of DLs, the solution of Eq. (3) gives in the simplest case, taking the CDW driving force $\mathcal{F}(j_c)$ to be linear,

$$q = \pi \frac{J_0 \lambda}{D_n g} \left[\exp\left(-\frac{|x + a|}{\lambda}\right) - \exp\left(-\frac{|x - a|}{\lambda}\right) \right], \tag{4}$$

with the contacts at $x = \pm a$. J_0 is the current applied at the contacts, λ the characteristic length scale of the phase slip distribution, and $D_n = \sigma_n l^2$ the normal carrier diffusion coefficient with l the normal carrier screening length. Equation (4) shows that for a long enough sample there will be no linear gradient in the central part of the sample. The carrier conversion will be complete, and the CDW deformation will be reduced to zero.

Applying Eq. (4) to our dc data, one obtains a very satisfying fit of the spatial variation of $q_{\pm}(x)$ from the contact position $x = 0$ to $x = 0.5$ mm with the characteristic length scale of the phase slip distribution $\lambda = 375 \pm 50$ μm (at $I_{\mathrm{CDW}} = 2.1 I_T$). However, the observed linear variation of q in the central part of the sample (Fig. 3) suggests that the conversion rate may be suppressed by pinning of the DLs, below some finite nonequilibrium threshold η_t: $\mathcal{R} = 0$ if $|\eta| < \eta_t$. In this latter case, the carrier conversion is blocked, and the normal and collective current densities, j_n and j_c, are fixed at values above (j_n) or below (j_c) their equilibrium values. We then see from Eq. (3) that $\partial\eta/\partial x = \eta' = \text{const} \neq 0$, thus $\eta(x) = \eta' x$, and therefore $q \propto x$, in agreement with the data in Fig. 3. More generally, numerical simulations of stationary solutions of Eq. (3) can be obtained for various types of conversion mechanisms and for the j_c dependence of $\mathcal{F}(j_c)$ obtained from experimental *I-V* curves [20].

The conclusions we derive from our high resolution x-ray measurements and from the above qualitative theoretical statements are as follows: for a long enough sample the large $q(x)$ values near the contacts decrease exponentially (in the simplest case) towards zero at the sample's center. The large gradients observed in earlier multicontact studies [16] can now be reinterpreted as due to an extreme size effect: the distance between contacts is so short that only a small part of the applied normal current is converted, so that the currents j_c and j_n stay far from their equilibrium values. In such a case, Eq. (4) is close to linear with only small contact increments. In contrast, earlier x-ray experiments [17], performed on longer samples (4.5 mm) could not resolve the contact region and what was observed as a bulk gradient coincides with our remnant distortion q_0' from pinned deformations.

An important observation is the fact that this gradient does not change between dc and pc experiments, indicating that the associated deformation is quenched. A related pinning phenomenon is observed in the *contact* region in *pulsed* experiments. Noting that 99% of the x-ray intensity is accumulated during the passive intervals between current pulses, we conclude that the observed pc shifts correspond to pinned deformations, which remain quenched on the time scale of the pulse interval. At very long times, thermal climb, similar to vortex creep, will allow for DL propagation and for the eventual decay of the deformation. Our preliminary results on the dependence of q on pulse frequency are in favor of this scenario.

The authors are indebted to M. Brunel (Cristallographie/CNRS) for making possible the x-ray characterization of the samples and to H. Berger and F. Levy (EPFL Lausanne) for providing the $NbSe_3$ samples. S. B. and N. K. have been partly supported by the Los Alamos R&D funds under the auspices of the U.S. DOE.

[1] P. W. Anderson, *Basic Notions of Condensed Matter Physics* (Benjamin Cummings, New York, 1984).
[2] J. S. Langer and V. Ambegoakar, Phys. Rev. **164**, 498 (1967).
[3] B. I. Ivlev and N. B. Kopnin, Adv. Phys. **33**, 47 (1984).
[4] E. Varoquaux and O. Avenel, Physica (Amsterdam) **197B**, 306 (1994).
[5] *Charge Density Waves in Solids*, edited by L. P. Gorkov and G. Grüner, Modern Physics in Condensed Matter Science Vol. 25 (North-Holland, Amsterdam, 1989).
[6] Special issue on Electronic Crystals, edited by S. Brazovskii and P. Monceau [J. Phys. IV (France) **3**, C2 (1993)].
[7] G. Grüner, *Density Waves in Solids* (Addison-Wesley, Reading, 1994).
[8] L. P. Gor'kov, JETP Lett. **38**, 87 (1983).
[9] N. P. Ong and K. Maki, Phys. Rev. B **32**, 6582 (1985).
[10] J. C. Gill, J. Phys. C **19**, 6589 (1986); in Ref. [6], p. 165.
[11] For a review, see F. Ya. Nad', in Ref. [5], p. 193.
[12] M. E. Itkis, F. Ya. Nad', and V. Ya. Pokrovskii, Sov. Phys. JETP **63**, 177 (1986).
[13] M. E. Itkis, B. M. Emerling, and J. W. Brill, Phys. Rev. B **52**, R11 545 (1995).
[14] M. C. Saint-Lager, P. Monceau, and M. Renard, Europhys. Lett. **9**, 585 (1989).
[15] M. E. Itkis, F. Ya. Nad', P. Monceau, and M. Renard, J. Phys. Condens. Matter **5**, 4631 (1993).
[16] T. L. Adelman *et al.*, Phys. Rev. B **53**, 1833 (1996), and references therein.
[17] D. DiCarlo *et al.*, Phys. Rev. Lett. **70**, 845 (1993).
[18] E. Canadell *et al.*, Inorg. Chem. **29**, 1401 (1990).
[19] S. Ramakrishna *et al.*, Phys. Rev. Lett. **68**, 2066 (1992).
[20] S. Brazovskii and N. Kirova (to be published).
[21] S. Brazovskii, J. Phys. I (France) **3**, 2417 (1993); also in Ref. [6], p. 267.
[22] S. Artemenko and A. Volkov, in Ref. [5], p. 365.
[23] K. Maki, Phys. Lett. A **202**, 313 (1995).